2011 IEEE International Conference on Rehabilitation Robotics
Rehab Week Zurich, ETH Zurich Science City, Switzerland, June 29 - July 1, 2011

Design of a Rotary Passive Viscoelastic Joint for Wearable Robots

Giorgio Carpino, Dino Accoto, Michelangelo Di Palo, Nevio Luigi Tagliamonte, Fabrizio Sergi, Eugenio Guglielmelli
Università Campus Bio-Medico di Roma
Laboratory of Biomedical Robotics and Biomicrosystems
Rome, Italy

Abstract— **In the design of wearable robots that strictly interact with the human body and, in general, in any robotics application that involves the human component, the possibility of having modular joints able to produce a viscoelastic behaviour is very useful to achieve an efficient and safe human-robot interaction and to give rise to emergent dynamical behaviors. In this paper we propose the design of a compact, passive, rotary viscoelastic joint for assistive wearable robotics applications. The system integrates two functionally distinct sub-modules: one to render a desired torsional stiffness profile and the other to provide a desired torsional damping. Concepts and design choices regarding the overall architecture and the single components are presented and discussed. A viscoelastic model of the system has been developed and the design of the joint is presented.**

Keywords: viscoelastic joint; wearable robots; pHRI.

I. INTRODUCTION

In the design of robots intended to strictly interact with humans the paradigm applied to traditional industrial robots "the stiffer is the better" [1] has been substituted by the concepts of compliance and adaptability. The development of robots that can establish dynamic interactions with the human body requires the use of joints and actuators which mechanical impedance can be adjusted (i.e. VIJ, Variable Impedance Joints and VIA, Variable Impedance Actuators). The tuning of the mechanical impedance, which is usefully exploited to perform different tasks, allows improving the dynamical performances of a joint, similarly to the variation of human joints stiffness [2].

The possibility of tuning the dynamical properties of the robotic systems is even more crucial in the design of Wearable Robots (WRs) for lower limbs in strict contact with the Human Body (HB). Compliant elements can be exploited so to cause the bouncing of mechanical energy between WR and HB during different phases of the gait cycle, reducing the WR actuation requirements. In this way the robot does not move rigidly the limbs of the subject through a prescribed pattern, but it offers assistance as needed (AAN) [3] or produces dynamical behaviours which aim to be very close to physiological movements. The proper implementation of such concepts leads to a safer pHRI (physical Human Robot Interaction), necessary condition for robots intended for assistive or rehabilitation purposes.

Joints compliance can be either achieved by *actively* controlling a stiff actuator so to mimic elastic behaviour, or by employing passive elements. The first example of a passive compliant actuator is the Series Elastic Actuator (SEA) [4] in which a spring is connected in series between the gear motor and the load to obtain an intrinsic impedance. This approach provides the possibility of storing energy, attenuating impacts and improving safety. The first SEA [4] was a linear actuator but a number of rotary SEA prototypes have been developed in recent years [5-10]. Those actuators adopt different solutions to implement the torsional elastic element. In [5] a frameless motor and hollow gear transmission are used and a spandrel-shape torsional spring is passed back through the center of the actuator; in [6] six linear springs with a three-spoke shaft are used; in [7] a similar approach is followed with 4 springs; in [8] two linear compression springs are connected to the actuator disk with a cable so that a torsional spring is created; in [9-10] a custom-made double spiral spring in series to a frameless motor is presented.

Solutions where the stiffness of passive elements can be modulated allow achieving both high energetic efficiency and a safer pHRI. This approach is referred to as Variable Stiffness Actuation (VSA) or, more in general, Variable Impedance Actuation (VIA). Regarding variable stiffness actuators a substantial number of designs have been developed [11-17].

All the proposed approaches are not capable to tune via hardware both stiffness and damping of the joint; they rely on the control for what concerns damping regulation.

This paper presents the design of a compact, passive, rotary viscoelastic joint. In section II the requirements for the system are listed; in section III the joint model is presented, while in section IV details on the design choices are provided. Conclusions and future works are discussed in section V.

II. REQUIREMENTS

The authors' aim is to design a modular robotic joint with intrinsic viscoelastic properties, which components can be

easily substituted, in order to comply with the requirements of different operative conditions.

Since the joint has to be compact and lightweight because it is intended for assistive WRs applications, the dimensional constraints for the joint were 150 mm for the diameter and 100 mm for the thickness and a maximum of 1.5 kg for the weight.

Taking into account the viscoelastic properties of the human joints, the output passive joint stiffness has to vary from 0 to 130 Nm/rad, the damping from 0 to 2 Nm•s/rad and the maximum input torque has to be 50 Nm.

III. Concept and Dimensioning

The goal of this work is to design a robotic viscoelastic rotary joint to be used in WRs applications. The joint has interchangeable modular components to provide different torque-displacement and torque-velocity characteristics, adaptable to a wide range of operative conditions.

The two sub-modules for the torsional spring and damper will be described in the next sections.

A. Torsional stiffness

The torsional stiffness module is implemented using n linear compression springs connected between the joint shaft and n rollers sliding on cam profiles. This arrangement generates a centering elastic torque $M(\theta)$ against an external rotation of the joint shaft. A desired stiffness characteristic can be achieved by opportunely selecting the shape of the cam.

In Fig. 1 a schematic representation of the stiffness module is depicted (only one spring k_m is represented).

The objective of this section is to derive the analytical expression for the cam profile $r(\theta)$ necessary to implement a generic torsional stiffness $k_\theta = f(\theta)$. In particular, the cases of constant, linear and quadratic torsional stiffness will be analyzed. The following analysis will consider the radius of the cam follower rollers in contact with the cam profile negligible.

A joint rotation θ causes a compression $x(\theta)$ of each spring, characterized by a stiffness k_m. The relation between the cam profile and the spring deformation can be expressed as:

$$r(\theta) = r_0 - x(\theta), \quad -\frac{\pi}{n} < \theta < \frac{\pi}{n} \tag{1}$$

where r_0 is the spring rest position.

Since $dM = k_\theta(\theta)d\theta$, the external moment can be written as:

$$M(\theta) = \int_0^\theta k_\theta(\alpha)\,d\alpha \tag{2}$$

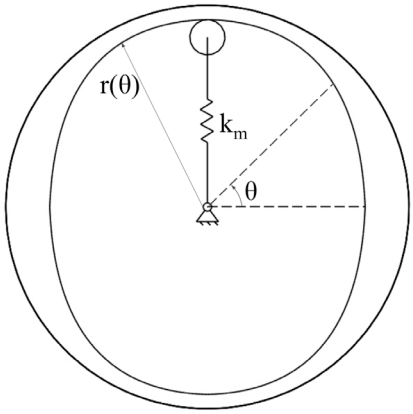

Figure 1. Schematic representation of the torsional spring module: k_m is the spring stiffness, θ the shaft rotation and $r(\theta)$ the cam profile.

The infinitesimal external work is $dL = M(\theta)d\theta$ and the total work associated to the compression of a spring is:

$$L(\theta) = \int_0^\theta M(\alpha)\,d\alpha \tag{3}$$

Moreover, the variation in the elastic energy of the n springs can be calculated as:

$$E(\theta) = n\int_0^{x(\theta)} k_m x(\alpha)\,dx \tag{4}$$

The energy balance $L(\theta)=E(\theta)$ leads to:

$$\int_0^\theta M(\alpha)\,d\alpha = n\int_0^{x(\theta)} k_m x(\alpha)\,dx \tag{5}$$

Equation (5) can be rewritten as:

$$\int_0^\theta M(\alpha)\,d\alpha = n\int_0^{x(\theta)} k_m x(\alpha)\frac{dx}{d\alpha}\,d\alpha \tag{6}$$

Calculating the derivative of (6) with respect to θ and using the expression (2) for the total moment, it can be obtained:

$$\int_0^\theta k_\theta(\alpha)\,d\alpha = nk_m x(\theta)\frac{dx}{d\theta} \tag{7}$$

Equation (7) can be readapted as:

$$\frac{1}{2}\frac{d(x^2(\theta))}{d\theta} = \frac{\int_0^\theta k_\theta(\alpha)\,d\alpha}{nk_m}, \tag{8}$$

From (8) the analytic relation between the torsional stiffness k_θ and the linear spring deflection can be derived as:

$$x(\theta) = \sqrt{\frac{2}{nk_m}\int_0^\theta d\alpha \int_0^\theta k_\theta(\alpha) d\alpha} \tag{9}$$

Considering a constant torsional stiffness k_θ, the resultant cam profile, taking into account (1), is:

$$r(\theta) = r_0 - \sqrt{\frac{k_\theta}{nk_m}}\theta \tag{10}$$

In case the torsional stiffness is $k_\theta(\theta) = A\theta$ (linear characteristic), the resultant cam profile is:

$$r(\theta) = r_0 - \sqrt{\frac{A}{3nk_m}}\theta^{1.5} \tag{11}$$

If the torsional stiffness is $k_\theta(\theta) = B\theta^2$ (quadratic characteristic), the resultant cam profile is:

$$r(\theta) = r_0 - \sqrt{\frac{B}{6nk_m}}\theta^2 \tag{12}$$

The corresponding cam profiles for the above mentioned characteristics are reported in the polar diagram of Fig. 2.

B. *Torsional damping*

The working principle is similar to a peristaltic pump: the torsional damping module is implemented connecting the joint shaft to a roller, which compresses a tube filled with a viscous fluid. The rotation of the shaft produces the motion of the fluid in the tube. Localized pressure drops, obtained by partially closing a valve, cause viscous forces which result, if the flow inside the tube is laminar, in a torque proportional to the angular velocity on the joint shaft.

A schematic representation of this module is reported in Fig. 3. With this arrangement the viscous damping can be varied modifying the pressure drop (i.e. varying the lumen of the tube through a valve). With the valve fully opened (minimal localized pressure drop), the minimal value of the torsional damping can be achieved.

In this section the equivalent torsional damping, as a function of geometric parameters of the system and of the rheological fluid properties, will be derived in the hypothesis of no localized pressure drop.

Assuming a laminar flow in the tube, for Poiseuille law the volumetric flow rate q can be written as:

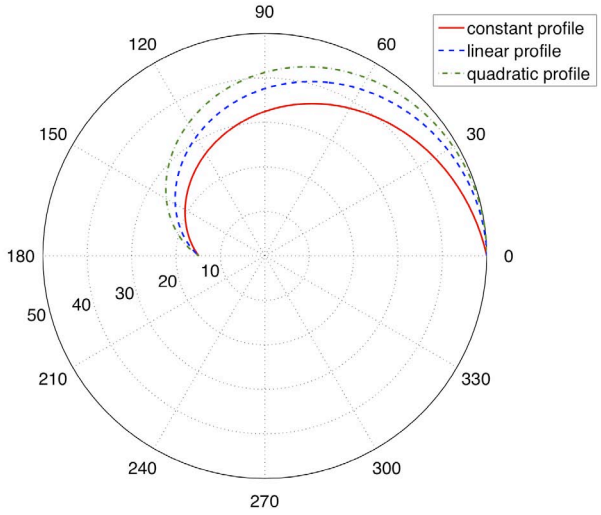

Figure 2. Cam profile for constant (solid line), linear (dashed line) and quadratic (dash-dot line) torsional stiffness characteristic. All the numbers in the graph are in mm.

$$q = \frac{\pi}{128\mu}\frac{\Delta p}{L}D^4 \tag{13}$$

where Δp is the pressure drop, μ the dynamic viscosity of the fluid, D the tube inner diameter, $L = 2\pi R$ the tube length with R the radius of curvature of the center line, as shown in Fig. 3. The power dissipated by fluid internal friction can be expressed as:

$$P_f = q\Delta p \tag{14}$$

The power associated to the rotation of the joint is:

$$P_j = c_{\min}\omega^2 \tag{15}$$

where c_{min} is the minimum viscous torsional damping and ω the joint angular velocity. For the energy conservation, $P_f = P_j$. From this equality it is possible to calculate the viscous damping as:

$$c_{\min} = \frac{q\Delta p}{\omega^2} \tag{16}$$

Considering the fluid mean linear velocity v and the tube section S, the volumetric flow can be written as:

$$q = vS = \omega R\frac{\pi}{4}D^2 \tag{17}$$

and the angular velocity can be obtained:

$$\omega = \frac{4q}{\pi RD^2} \tag{18}$$

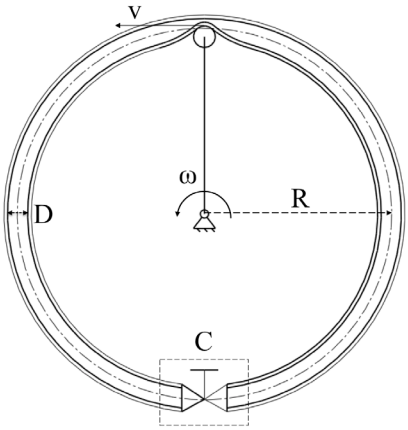

Figure 3. Schematic representation of the torsional damping module. ω is the angular velocity, R the radius, D the inner diameter of the tube and v the linear velocity. The valve is schematized in block C.

Substituting the quantity $\Delta p/q$ (calculated from (13)) and (18) in (16), the minimal torsional damping can be calculated as:

$$c_{\min} = 16\pi^2 \mu R^3 \tag{19}$$

The obstruction of the tube, obtained by the action of the valve C in Fig. 3, increases the viscous drop in the system with a consequent increase of the value of the torsional damping c.

IV. Design

This section describes the design of the joint. The presented design has a 115 mm diameter and 85 mm thickness with a weight of 1.4 kg.

A. Torsional stiffness module

The torsional spring is implemented using a roller with a spring support following a cam profile.

The system, shown in Fig. 4, is comprised of a central hub (AISI 420) connected to shaft through a key, four self-lubricating bushings, four harmonic steel springs, four rollers-springs connectors, four cam follower rollers, and the cam profile (AISI 420).

The shaft is simply supported by two radial ball bearings. The central hub has two holes to connect the fluid mover system of the torsional damping module.

The self-lubricating bushings (MU - Boccole Italia Srl) have a twofold function: hosting the springs so to reduce the friction between the rollers-springs connectors and the central hub; avoiding bending moments on the spring which can produce undesired compression forces outside the axis of the springs. The rollers-springs connectors (AISI 420) support the cam follower rollers.

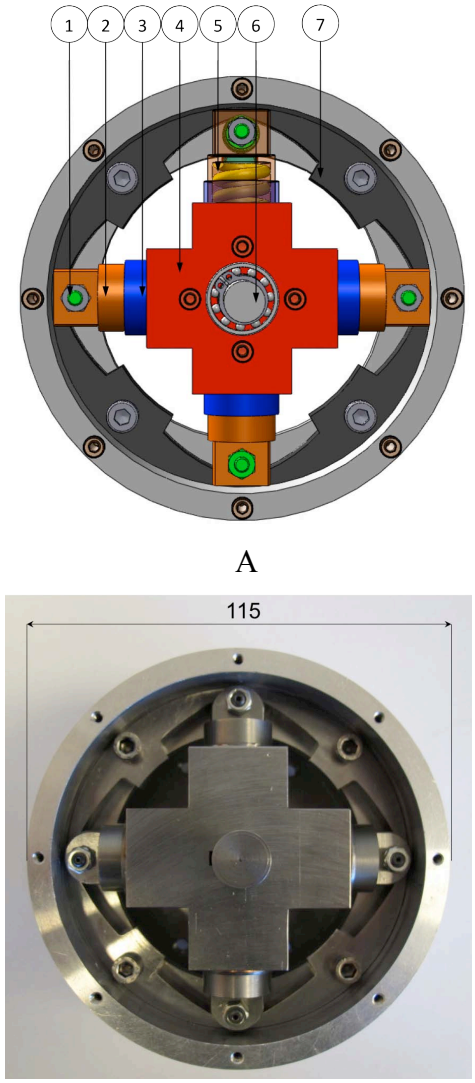

Figure 4. (A) 3D CAD drawing of the tosional spring module (constant stiffness and 4-springs configuration is reported). 1: cam follower rollers, 2: rollers-springs connectors, 3: bushings, 4: central hub, 5: linear compression springs, 6: central shaft, 7: cam profiles. (B) Frontal view of the prototype highlighting the components of the torsional stiffness module with diameter dimension overlaid (mm).

TABLE I. Springs Main Characteristics

Springs Characteristics	Values
Outer diameter	15.5 mm
Inner diameter	9.1 mm
Wire diameter	3.1 mm
Length	25 mm
Pitch	5.37 mm
Weight	12.77 g
Number of coils	5.5
Stiffness	140.9 N/mm
Block lenght	18.6 mm
Material	DIN 172233, C1 class

The main characteristics of the springs are reported in Table 1. The cam profile is intended in this case for constant torsional stiffness but, as discussed above, it can be replaced with different cam profiles able to produce a linear or quadratic characteristic for the torsional stiffness.

In Fig. 5 a plot for the three possible stiffness characteristics (constant, linear and quadratic) are reported. The maximum rotation is reached when the springs go in block. A maximum rotation of ±60° can be achieved for the case of quadratic stiffness in a 3-springs configuration, as it is clear in Fig. 5. Considering instead a 4-springs configuration, the resulting maximum rotation would be ±45°.

Table II summarizes all the results in terms of stiffness, number of springs, maximum rotation, maximum torque and maximum elastic energy for constant, linear and quadratic torsional stiffness characteristics.

B. *Torsional damping module*

The damping module, depicted in Fig. 6, includes a silicone tube set in circular configuration (radius R = 50 mm) and fixed to the chassis (Anticorodal Al 6000). The tube is filled with water and it is provided with a screw, which forces the stricture of the lumen so to produce a localized pressure drop. The silicone tube has an outer diameter of 8 mm and an inner diameter of 5 mm. When the tube is completely open (laminar flow, Reynolds number equal to 750), the torsional damping is minimum ($1.97 \cdot 10^{-5}$ Nm·s/rad) as calculated in Section III.B. The elements of the damping module have been designed in order to obtain a minimum damping much lower than the desired output damping. When the tube is completely obstructed the torsional damping can theoretically become infinite. The fluid mover (Anticorodal Al 6000) has an adjustable arm, which allows the shift of the roller for an easy insertion/substitution of the tube.

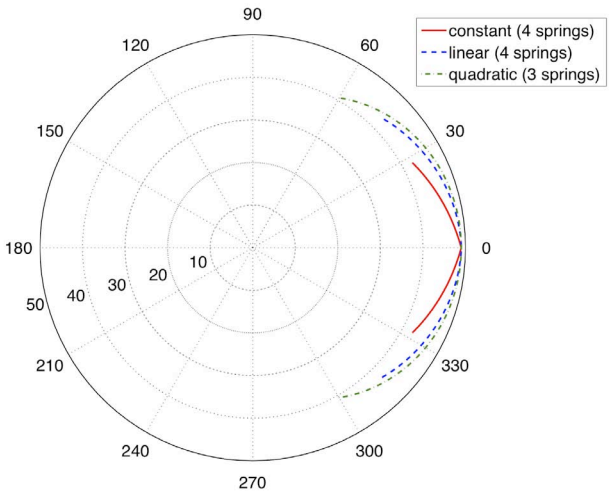

Figure 5. Resultant cam profile for for constant (solid line), linear (dashed line) and quadratic (dash-dot line) torsional stiffness. All the numbers in the graph are in mm.

TABLE II. RESULTS FOR CONSTANT, LINEAR AND QUADRATIC TORSIONAL STIFFNESS CHARACTERISTICS.

	Torsional Stiffness		
	Constant $k_\theta(\theta)=K$	***Linear*** $k_\theta(\theta)=A\theta$	***Quadratic*** $k_\theta(\theta)=B\theta^2$
Stiffness	K = 100 Nm/rad	A = 125 Nm/rad	B = 96.1 Nm/rad
Springs number	4	4	3
Max. rotation	± 28°	± 45°	± 60°
Max. torque	48 Nm	40 Nm	34 Nm
Max. total elastic energy	12 J	10.7 J	8.7 J

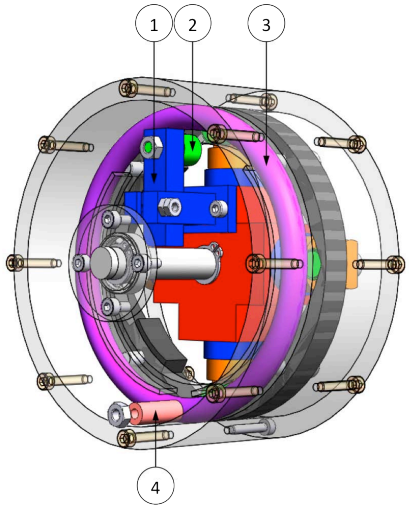

A

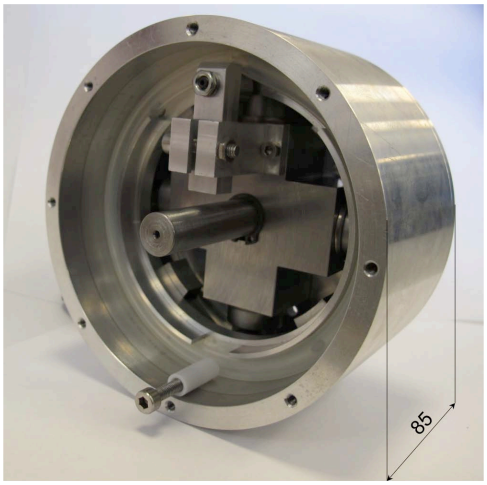

B

Figure 6. (A) 3D CAD drawing of torsional damping module. 1: fuid mover, 2: cam follower roller, 3: silicone tube, 4: pressure drop regulator. (B) View of the prototype highlighting the components of the torsional damping module with thickness dimension overlaid (mm).

V. Conclusions and Future Works

In this paper the design of a compact, lightweight, rotary viscoelastic joint for wearable robotics applications is presented. The model of the system is developed and the design is presented. All the requirements reported in section II are fulfilled.

The presented design is endowed with a high degree of modularity, which enables the regulation of the mechanical properties of the system by replacing single components. For example, the modification of the stiffness vs. angle characteristic can be achieved by using a different cam profile or by employing linear springs with different elastic constants. Moreover, damping can be varied by using different fluids and/or by regulating the localized pressure drop in the tube.

The presented joint is intended to be passive but it can be easily actuated to obtain a Series Visco-Elastic Actuator (SVEA). This can allow having a tunable physical damping component instead of rendering a viscous behavior via impedance control.

The presented joint can be used in WRs for rehabilitation and assistance, and in all the applications where a safe pHRI is crucial. Humanoid and walking robots can also benefit from viscoelastic joints for energetic efficiency and biomimetic behaviours.

Future works will be focused on the characterization of the system through a custom made test bed already developed.

Acknowledgment

This work was supported by the FP7 FET Proactive Initiative "Embodied Intelligence" of the European Commission, project no. ICT-2007.8.5-231451 - EVRYON (EVolving morphologies for human-Robot sYmbiotic interactiON).

References

[1] K. Salisbury, B. Eberman, M. Levin, W. Townsend, "The Design and Control of an Experimental Whole-Arm Manipulator", International Symposium on Robotic Research, pp. 233-241, 1991.

[2] A. Bicchi and G. Tonietti, "Fast and Soft-Arm Tactics - Dealing with the Safety-Performance Tradeoff in Robot Arms Design and Control", IEEE Robotics & Automation Magazine, vol. 11(2), pp. 22–33, 2004.

[3] H. Vallery, J. Veneman, E. Van Asseldonk, R. Ekkelenkamp, M. Buss, H. Van der Kooij, "Compliant Actuation of Rehabilitation Robots", IEEE Robotics & Automation Magazine, vol. 15(3), pp. 60–69, 2008.

[4] G. A. Pratt, M. M. Williamson, "Series Elastic Acutators", Proceedings of the International Conference on Intelligent Robots and Systems, vol. 1, pp. 399-406, 1995.

[5] J. W. Sensinger, R. F. Weir, "User-Modulated Impedance Control of a Prosthetic elbow in Unconstrained, Perturbed Motion", IEEE Transactions on biomedical engineering, vol. 55, pp. 1043– 1055, 2008.

[6] N. G. Tsagarakis, M. Laffranchi, B. Vanderborght, D. G. Caldwell, "A compact soft actuator unit for small scale human friendly robots", IEEE International Conference on Robotics and Automation, Kobe, Japan, pp. 4356–4362, May 2009.

[7] G. Wyeth, "Demonstrating the safety and performance of a velocity sourced Series Elastic Actuator", IEEE International Conference on Robotics and Automation, Pasadena, CA, USA, pp. 3642-3647, May 2008.

[8] J. F. Veneman, R. Ekkelenkamp, R. Kruidhof, F. C.T. van der Helm and H. van der Kooij, "A Series Elastic- and Bowden-Cable-Based Actuation System for Use as Torque Actuator in Exoskeleton-Type Robots", The international journal of robotics research, vol 25(3), pp. 261–281, 2006.

[9] A. H. A. Stienen, E. E. G. Hekman, H. ter Braak, A. M. M. Aalsma, F. C. T. van der Helm, H. van der Kooij, "Design of a Rotational Hydroelastic Actuator for a Powered Exoskeleton for Upper Limb Rehabilitation", IEEE Transactions on biomedical engineering, vol. 57(3), pp. 728-735, 2010.

[10] C. Lagoda, A. H. A. Stienen, E. E. G. Hekman, H. van der Kooij, "Design of an electric Series Elastic Actuated Joint for robotic gait rehabilitation training", IEEE International Conference on Biomedical Robotics and Biomechatronics, Tokyo, Japan, pp. 21-26, September 2010.

[11] G. Tonietti, R. Schiavi, A. Bicchi, "Design and Control of a Variable Stiffness Actuator for Safe and Fast Physical Human/Robot Interaction", IEEE International Conference on Robotics and Automation, pp. 528–533, 2005.

[12] R. Schiavi, G. Grioli, S. Sen, A. Bicchi, "VSA-II: a Novel Prototype of Variable Stiffness Actuator for Safe and Performing Robots Interacting with Humans", IEEE International Conference on Robotics and Automation, Pasadena, CA, USA, pp. 2171–2176, May 2008.

[13] J. Choi, S. Hong, W. Lee, S. Kang, "A variable stiffness joint using leaf springs for robot manipulators", IEEE International conference on Robotics and Automation, Kobe, Japan, pp. 4363–4368, May 2009.

[14] S. Wolf and G. Hirzinger, "A New Variable Stiffness Design: Matching Requirements of the Next Robot Generation: Matching Requirements of the Next Robot Generation," IEEE International Conference on Robotics and Automation, Pasadena, pp. 1741-1746, 2008.

[15] B. S. Kim, J. J. Park, J. B. Song, "Double Actuator Unit with Planetary Gear Train for a Safe Manipulator," IEEE International Conference on Robotics and Automation, Rome, pp: 1146-1151, 2007.

[16] J. W. Hurst, J. E. Chestnutt, A. A. Rizzi, "An Actuator with Physically Variable Stiffness for Highly Dynamic Legged Locomotion", International Conference on Robotics and Automation, New Orleans, LA, 2004.

[17] N. L. Tagliamonte, F. Sergi, G. Carpino, D. Accoto, E. Guglielmelli, "Design of a Variable Impedance Differential Actuator for Wearable Robotics Applications", IEEE/RSJ International Conference on Intelligent Robots and Systems, Taipei, Taiwan, pp. 2639-2644, October 2010.